catalysts

MDPI

Article

Photocatalytic Mineralization of Emerging Organic Contaminants Using Real and Simulated Effluents in Batch and Membrane Photoreactors

Cristina Lavorato [1,*], Angela Severino [1], Pietro Argurio [1], Raffaele Molinari [1,*], Beatrice Russo [2], Alberto Figoli [2] and Teresa Poerio [2]

[1] Department of Environmental Engineering (DIAm), University of Calabria, Via P. Bucci, Cubo 44/A, 87036 Rende, Italy; angela.severino@unical.it (A.S.); pietro.argurio@unical.it (P.A.)
[2] Institute on Membrane Technology, National Research Council, ITM-CNR, Via P. Bucci, Cubo 17/C, 87036 Rende, Italy; b.russo@itm.cnr.it (B.R.); a.figoli@itm.cnr.it (A.F.); t.poerio@itm.cnr.it (T.P.)
* Correspondence: cristina.lavorato@unical.it (C.L.); raffaele.molinari@unical.it (R.M.)

Abstract

Conventional wastewater treatment plants (WWTPs) have limited efficiency in removing emerging pollutants (EPs), meaning these pollutants persist and lead to widespread ecological contamination. In this study, real effluents from a WWTP were characterized using TOC and Py-GC/MS, which indicated the presence of various organic compounds that could be indicative of micro-nanoplastics (MNPs) or plastics additives. To address this challenge, we propose the use of a photocatalytic membrane reactor (PMR) as an advanced treatment system capable of achieving high degradation efficiency under mild operating conditions. Preliminary experimental tests were conducted using various commercial photocatalysts (TiO_2, WO_3, Nb_2O_5), four UV lamps, and oxidants (air, O_2) using added Gemfibrozil (GEM) as a drug model compound. Real effluent samples collected from WWTP were tested with and without pretreatment to remove coarse particles prior to photocatalysis. Mineralization was achieved in both cases, but it occurred at a higher rate for the pretreated effluent. The mineralization of GEM and EPs in real effluent was achieved within five hours under UV irradiation using titanium dioxide (TiO_2) as a low-cost photocatalyst in a PMR. The results highlight the potential of photocatalytic systems, and particularly PMRs, as a promising technology for removing recalcitrant pollutants in real effluents offering a viable solution for improved environmental protection.

Keywords: photocatalysis; photocatalytic membrane reactor (PMR); wastewater treatment; micro-nanoplastics degradation; pollutants; gemfibrozil

check for updates

Academic Editor: Jorge Bedia

Received: 14 August 2025
Revised: 5 September 2025
Accepted: 11 September 2025
Published: 18 September 2025

Citation: Lavorato, C.; Severino, A.; Argurio, P.; Molinari, R.; Russo, B.; Figoli, A.; Poerio, T. Photocatalytic Mineralization of Emerging Organic Contaminants Using Real and Simulated Effluents in Batch and Membrane Photoreactors. *Catalysts* **2025**, *15*, 904. https://doi.org/10.3390/catal15090904

Copyright: © 2025 by the authors. Licensee MDPI, Basel, Switzerland. This article is an open access article distributed under the terms and conditions of the Creative Commons Attribution (CC BY) license (https://creativecommons.org/licenses/by/4.0/).

1. Introduction

Pollutant contamination of freshwater ecosystems has become an increasing environmental concern [1]. As the global population increases, the strategic importance of wastewater treatment in addressing shortages of drinking water has become more critical, both for economic sustainability and for public health [2]. One of the key challenges in managing water utility in industries is the disposal of wastewater [3]. The discharge of industrial effluents into water bodies contributes significantly to environmental degradation and poses serious risks to human and ecosystem health. To ensure environmental safety and the sustainability of resources, treated wastewater must meet stringent quality

standards for various applications, including discharge, reuse in industrial processes, irrigation and aquifer recharge [4]. It has been widely shown that conventional municipal wastewater treatment plants (WWTPs) are ineffective at removing many types of pollutants, particularly emerging organic contaminants (EOCs) [5–8]. Multiple studies have shown that municipal WWTPs in various countries may not fully remove plastic particles [9,10], as traces of microplastics have been detected in treated effluents, indicating their role as a pathway for micro-nanoplastics (MNPs) to enter aquatic environments [11]. An additional risk caused by MNPs is the release of plastic additives, such as phthalates, into water [12]. The widespread presence of MNPs across various environmental systems is concerning due to their potential impacts on both terrestrial and aquatic ecosystems, including the human food chain [13]. Once inside the human body, these particles may induce inflammation, oxidative stress, and cellular damage [14]. Emerging studies suggest potential impacts on the immune, endocrine, and reproductive systems [15]. However, further research is needed to fully understand the long-term health effects of human exposure to MNPs [16]. The findings highlight the urgent need for continued research and measures to reduce the environmental consequences of plastic pollution. Nanoplastics are increasingly recognized as emerging contaminants in wastewater and have the potential to act as vectors for pharmaceutical pollutants [17]. Rochman et al. reported bioaccumulation of chemicals and associated health effects from plastic ingestion in fish and demonstrate that future assessments should consider the complex mixture of the plastic material and their associated chemical pollutants [18]. Among these contaminants, pharmaceutical compounds such as gemfibrozil (GEM), a widely used lipid-regulating drug, was found in the influent and effluent at a wastewater treatment plant (WWTP) as well as in the groundwater below a land application site that received treated effluent from the WWTP [19]. Gemfibrozil (GEM) is among the most commonly found pharmaceuticals in surface water in concentrations ranging from 11 to 187 ng/L [20]. Incomplete removal during biological wastewater treatments is the main source of surface water contamination [21]. The combined presence of nanoplastics and pharmaceuticals such as GEM in real wastewater raises concerns about their simultaneous photocatalytic degradation. Fang et al. found gemfibrozil (GEM) in wastewater influent, effluent, and groundwater in the range of 3.47 to 63.8 μg/L, 0.08 to 19.4 μg/L, and undetectable to 6.86 μg/L, respectively. The simultaneous degradation of both MNPs and gemfibrozil has been chosen in this work to demonstrate the versatility of the proposed system against chemically different contaminants, which often coexist in real wastewater scenarios. Under aerobic conditions, dissipation half-lives for gemfibrozil in sandy loam and silt loam soils were 17.8 and 20.6 days, respectively; 25.4 and 11.3% of gemfibrozil was lost through biodegradation from the two soils over 14 days. Various drugs, such as GEM, can be toxic to aquatic organisms and lead to bioaccumulation along the aquatic food chain. This can pose a health risk to humans [22].

In general, pollutants are released into the environment within legal limits in very low concentrations, but they can accumulate in the environment or in humans and animals increasing the risk associated with their contamination. So, highly efficient wastewater treatment processes are required that include an advanced tertiary treatment stage to obtain higher water quality. A green method that could allow the complete mineralization of real effluent from wastewater treatment plants (RE-WWTPs) is photocatalysis. Advanced Oxidation Processes (AOPs) such as photocatalysis have emerged as promising technologies for the degradation of recalcitrant organic molecules and plastic materials [23–27]. Photon-driven activation is more environmentally friendly than thermal activation, as it allows the use of safer catalysts like TiO_2 and mild oxidants such as molecular oxygen, operating under ambient conditions [26]. While visible light is, generally, considered the greener option, even UV-driven photocatalysis has become increasingly sustainable thanks

to recent advances in energy technologies. The use of photovoltaic-powered UV lamps and solar concentrator systems can enable UV light sources to be powered by renewable energy [28,29]. Additionally, UV irradiation, despite its higher energy demand, offers greater photocatalytic efficiency and faster degradation rates. Combined with inexpensive and non-toxic photocatalysts like TiO_2, which are effective under UV without requiring noble metals or complex modifications, this makes UV- Heterogeneous Photocatalysis (UV-HPC) a powerful and viable sustainable technology. HPC also requires few additives, it can treat pollutants in various phases even at low concentrations, and it is compatible with other treatment methods. Photocatalysis has the potential to convert MNPs into harmless by-products such as carbon dioxide, water, and simple organic compounds. These characteristics make photocatalysis an attractive option as a low-cost, environmentally friendly, and sustainable solution for addressing various types of pollution [24,30]. Our research groups have previously investigated the photocatalytic degradation of microplastics, nanoplastics, and pharmaceutical contaminants [25,30,31]. In our previous works, we investigated the degradation of gemfibrozil in water by using different types of PMRs. In our recent studies, we developed an innovative approach for treating water contaminated with polyester fibers and polystyrene, combining membrane separation with photocatalytic processes [24,30]. We simulated polluted water containing micro-nanoplastic particles (MNPs), such as polyester fibers derived from a household dryer [30]. These ones were recovered with 98% efficiency using a membrane separation process employing polymeric membranes, followed by partial degradation or fragmentation into smaller particles. In a subsequent study, we simulated polluted water containing a low concentration of nanoparticles (NPs), specifically commercial polystyrene NPs with an average size of 150 nm [24]. In this case, we used tubular multichannel inorganic membranes, achieving 100% recovery and pre-concentration of the NPs prior to photocatalytic treatment. Complete mineralization was then obtained within 24 h using TiO_2 under UV irradiation. More recently, we demonstrated the removal and concentration of MNPs from municipal wastewater effluent, achieving a high volume-reduction factor (VRF) of 139 [11]. Nevertheless, a comprehensive investigation on the degradation of pollutants in a real effluent containing also gemfibrozil (added) gives more information on the effectiveness of the PMR, particularly in the presence of co-contaminants such as NPs and plasticizers in real wastewater effluents. This last sentence inspired the present work. In this context, photocatalytic membrane reactors (PMRs) can be very effective in the removal of organic pollutants (particularly recalcitrant compounds) from wastewater because they allow for the mineralization of organic pollutants to innocuous by-products, thus achieving high-quality treated water [23]. When photocatalysis is integrated with membrane systems [25,32–35], the overall performance of the system is enhanced: in PMRs, the presence of a photocatalyst (e.g., TiO_2) generates reactive oxygen species (ROS) under light irradiation. These ROS actively oxidize organic foulants on the membrane surface, thereby mitigating irreversible fouling, preserving membrane permeability, and reducing the frequency of chemical cleaning, addressing one of the main limitations of conventional membrane systems [36]. The combination of a membrane system with a photocatalytic reactor offers several advantages, including the ability to confine the photocatalyst, the target pollutants, and their oxidation products within the reaction environment, while simultaneously allowing the treated water to be collected as permeate.

In this work, a comprehensive set of experimental investigations was conducted to evaluate the photocatalytic degradation and mineralization of emerging pollutants under various operating conditions. Initially, batch experiments were carried out using gemfibrozil as a model pollutant to assess the influence of different commercial photocatalysts (TiO_2, WO_3, Nb_2O_5), light sources (UV-LED, mercury lamps, UVC), and oxidants (oxygen

vs. atmospheric air). Subsequently, we carried out the mineralization of real effluents from a wastewater treatment plant pretreated by membrane filtration to remove coarse particles and improve the efficiency of the photocatalytic treatment. These samples were characterized using total organic carbon (TOC) and pyrolysis–gas chromatography–mass spectrometry (Py-GC/MS) analyses, which indicated the presence of various organic compounds that may be indicative of MNPs and plastics additives. Photocatalytic degradation of both GEM and RE-WWTP were carried out in the PMR. The simultaneous degradation of both MNPs and gemfibrozil was chosen to demonstrate the versatility of the proposed system against chemically different contaminants, which often co-exist in real wastewater scenarios. This setup was explored to evaluate the potential of the oxidation process for the advanced treatment of wastewater and the production of high-quality effluent suitable for reuse.

2. Results and Discussion

2.1. Photocatalytic Gemfibrozil Degradation

Experimental tests were conducted in the batch reactor shown in Figure S4 to collect information on the operative conditions for the photocatalytic degradation of gemfibrozil for subsequent use in PMR. Photocatalytic degradation tests of GEM, a model pollutant, were performed in a batch reactor under Hg lamp irradiation and blowing oxygen as the oxidant. Based on their well-documented photocatalytic properties, stability, and prior use in environmental applications, particularly in oxidation and degradation reactions, the activity of different photocatalysts including TiO_2, WO_3 and Nb_2O_5 was compared [37–39]. As shown in Figure 1A, complete degradation of GEM was achieved using TiO_2 and WO_3 after 30 and 120 min, respectively. Although tungsten trioxide (WO_3) possesses strong oxidation potential and low toxicity and is widely used in photocatalysis and related applications [15–22], the lower photocatalytic activity under these experimental conditions was caused by its limited photocatalytic efficiency under UV light due to its narrower band gap (~2.5–2.7 eV), which favored absorption in the visible rather than UV range [40]. The mineralization was absent by using Nb_2O_5 (Figure 1B), indicating its poor photocatalytic performance under the tested conditions. To investigate if light scattering influenced negatively the photocatalytic activity of Nb_2O_5 during GEM degradation, additional experiments were carried out using lower photocatalyst concentration (0.5 g/L) compared with the previous, as shown in Figure 1C. The results indicated that varying the concentration of Nb_2O_5 had no significant effect on its photocatalytic performance and confirmed that pure titanium dioxide performs better than pure niobium pentoxide as reported in some cases [41].

In photocatalytic reactions, both the intensity and wavelength of light play crucial roles in determining the efficiency of the process. The intensity of the light source affects the rate of electron excitation within the photocatalyst, with higher intensities typically leading to a greater number of electron–hole pairs generated, thus enhancing the reaction rate. On the other hand, the wavelength of light is equally important because photocatalysts are often sensitive to specific wavelengths, corresponding to their bandgap energy. For instance, UV light, with shorter wavelengths, can provide the energy needed to excite electrons in many photocatalysts, while visible light, with longer wavelengths, may require catalysts designed to absorb this range of light. Different types of lamps, such as mercury vapor lamps, LEDs, or Xenon lamps, emit light at different intensities and wavelengths, making them more or less suitable for specific photocatalytic applications.

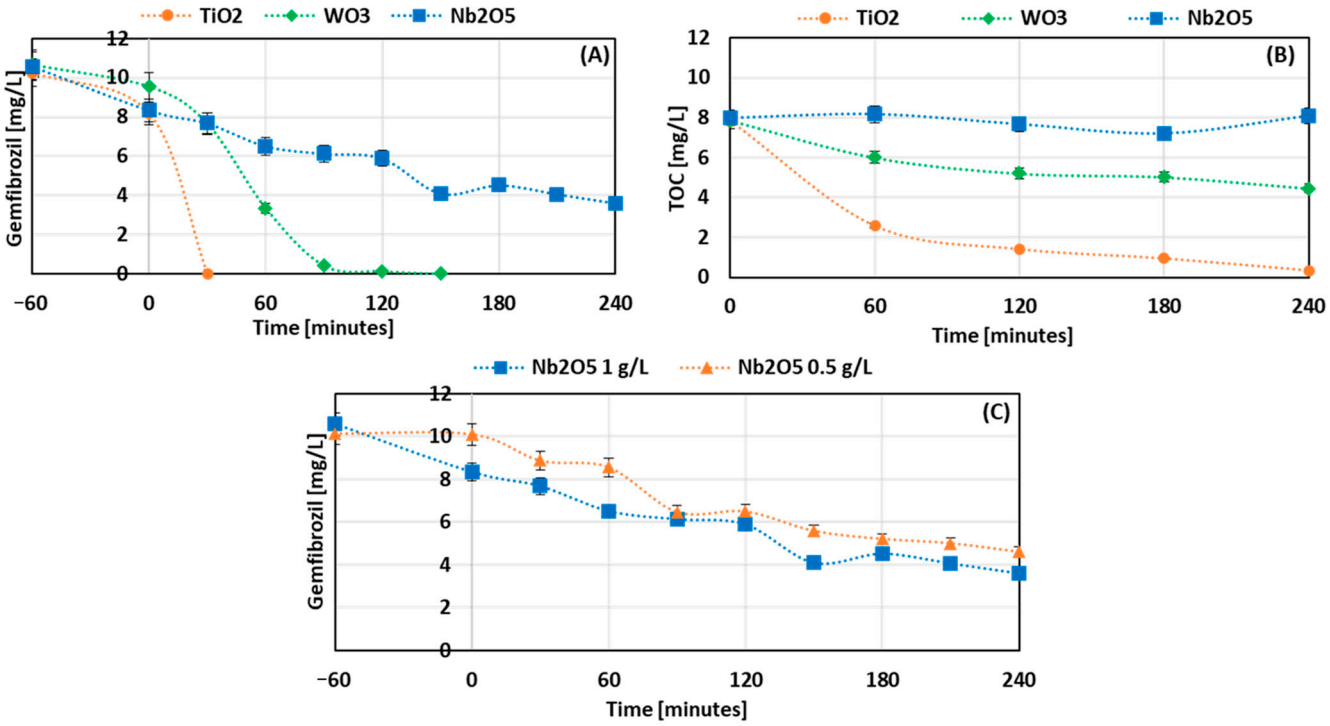

Figure 1. Comparison of (**A**) GEM degradation and (**B**) TOC vs. time using different photocatalysts; (**C**) comparison of GEM degradation vs. time using different amount of N_2O_5 as photocatalyst (operative conditions: V = 500 mL, 1 g/L of photocatalyst suspension in water, 10 mg/L GEM, T = 30 °C, oxygen pressure 0.5 bar, medium pressure Hg lamp A as irradiation source).

Therefore, the choice of lamp is crucial for optimizing the reaction conditions and improving the overall efficiency of the photocatalytic process. To this end, the photocatalytic degradation of gemfibrozil as a model pollutant was studied using different lamps with different intensities and wavelengths. Photolysis tests showed that almost no mineralization occurred in the absence of a photocatalyst (Figure S5).

A comparison of various lamp sources with different intensities and wavelengths on the photocatalytic degradation of GEM and TOC removal is presented in Figure 2A and 2B, respectively. The results demonstrated that the highest performance in both GEM degradation and mineralization was achieved using Hg medium pressure lamp B (7246 μW/cm^2) which led to complete degradation of GEM within 30 min and significant TOC reduction. Similarly, Hg lamp A (4785 μW/cm^2) also enabled full degradation of GEM within the same time frame. The emission spectrum of both lamps exhibited a main peak at 360 nm, along with additional peaks in both the UV and visible regions. Conversely, a marked decrease in performance was observed with lower-intensity sources. The LED lamp (105.59 μW/cm^2 with emission peak at 367 nm) required 150 min to achieve complete GEM degradation and showed limited mineralization, while the TUV mini UVC lamp (2.73 μW/cm^2 with main emission peak at 250 nm) exhibited minimal photocatalytic activity, with complete degradation reached only after 360 min and negligible TOC reduction, evidencing poor GEM mineralization. These findings highlight the importance of key parameters, including emission spectrum and irradiance, on photocatalytic activity, especially in relation to the specific catalyst employed. Such factors critically influence the degradation performance towards pharmaceutical and other organic pollutants in water treatment processes. While high-intensity lamps offer superior efficiency, lower-intensity alternatives like LEDs may be preferable in certain contexts due to their lower energy demand and operational costs.

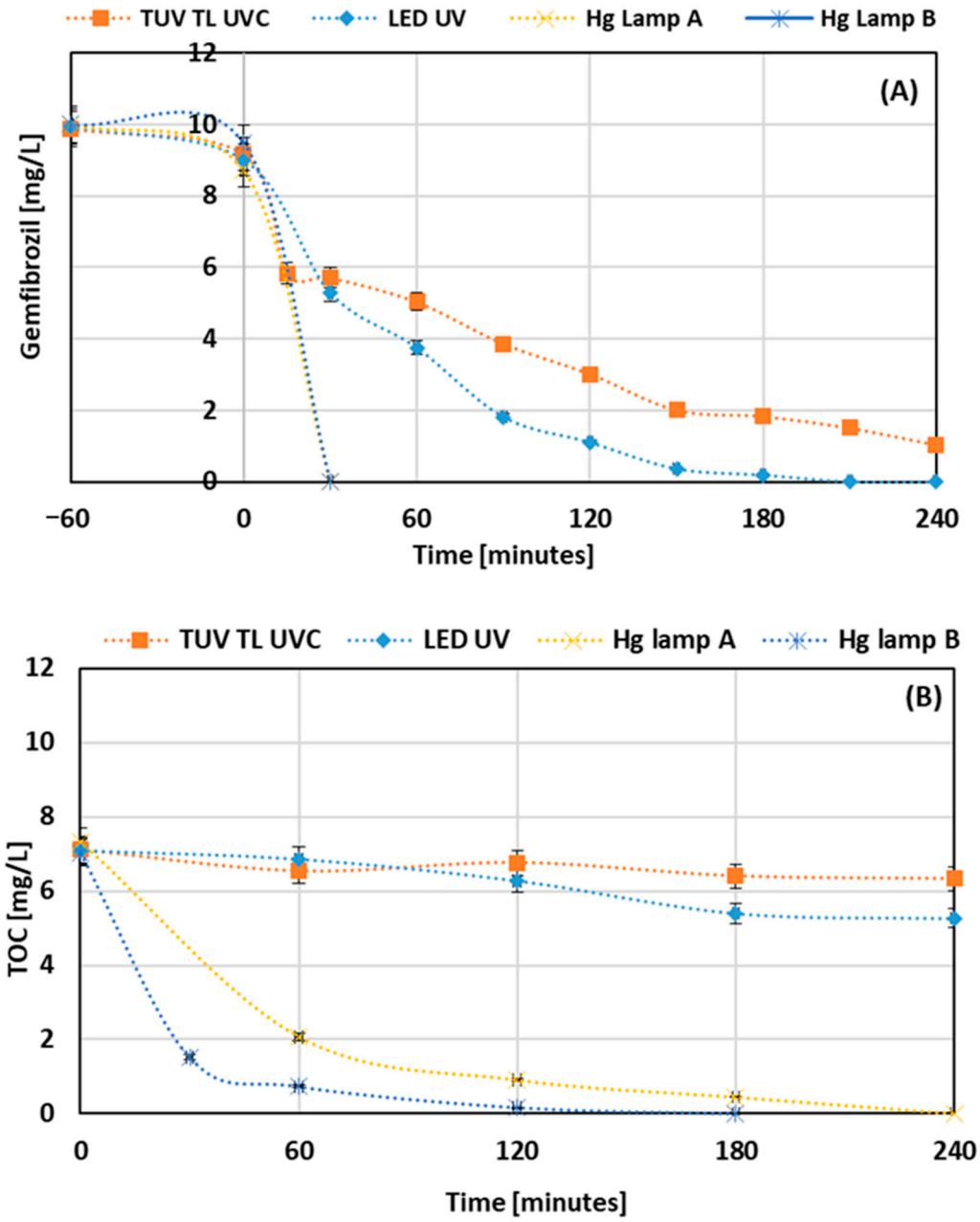

Figure 2. Comparison of (**A**) Gemfibrozil degradation and (**B**) TOC vs. time using different lamps (operative conditions: 500 mL, 1 g/L of photocatalyst suspension in water, 10 mg/L Gemfibrozil, 30 °C, oxygen pressure 0.5 bar).

Subsequent tests focused on the more efficient Hg lamp B, as it enabled shorter irradiation times compared to other available lamps. Additional photocatalytic experiments were carried out to evaluate the influence of molecular oxygen or atmospheric air as oxidizing agents (Figure 3). The presence of oxygen insufflation in the reaction environment resulted in a slightly higher photocatalytic efficiency compared to the use of atmospheric air as an oxidant.

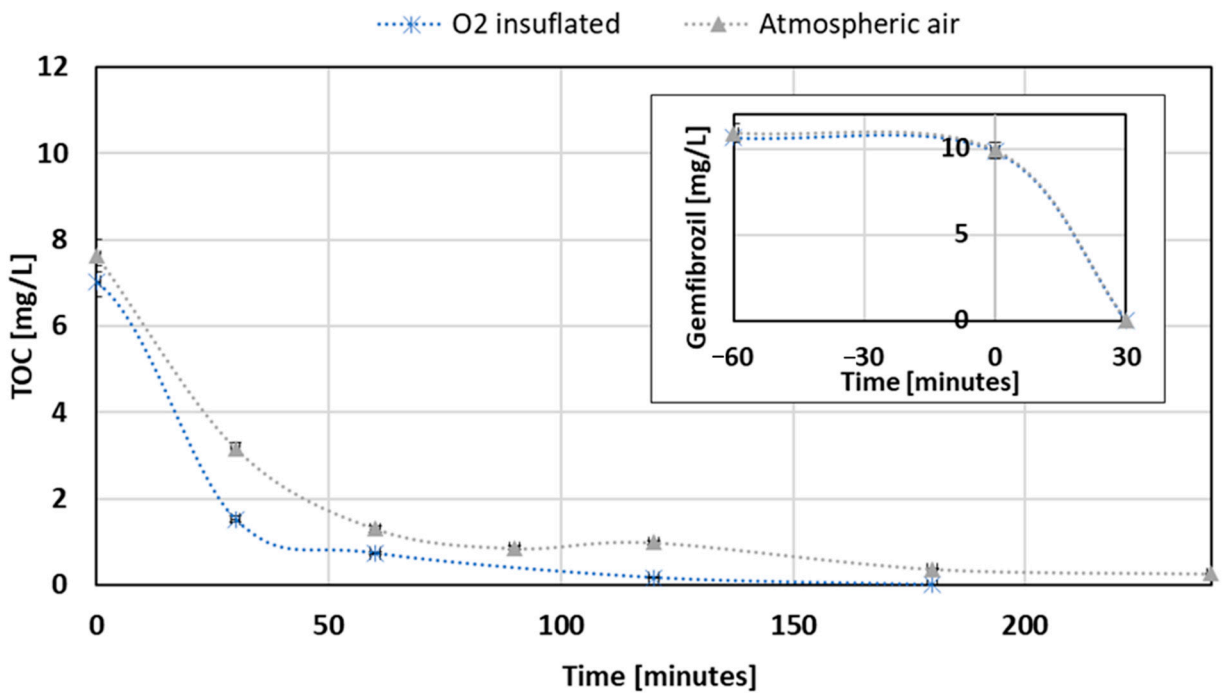

Figure 3. Gemfibrozil mineralization as TOC vs. time using oxygen at 0.5 bar or atmospheric air as oxidant. The inset reports the Gemfibrozil concentration vs. time in the same test (operative conditions: 500 mL, 1 g/L of TiO_2 as photocatalyst suspension in water, 10 mg/L Gemfibrozil, 30 °C, medium pressure Hg lamp B as irradiation source).

2.2. Real Effluent from Wastewater Treatment Plant

2.2.1. Characterization of RE-WWTP

In our study, we characterized real effluents from a wastewater treatment plant (RE-WWTP) collected during different periods, specifically in July 2024 (J) and November 2024 (N), using Py-GC/MS. The RE-WWTP samples were characterized by measuring pH values in the range of 7.900 ± 0.032; TOC and IC values were 6.313 ± 0.316 mg/L and 25.42 ± 1.27 mg/L, respectively, for the sample taken in November (RE-WWTPN), while they were 11.00 ± 0.55 mg/L and 26.34 ± 1.32 mg/L, respectively, for the sample taken in July (RE-WWTPJ); the conductivity was 829 and 803 µS/cm for RE-WWTPJ and RE-WWTPN, respectively, and the amount of suspended solids removed through filtration was on average 5 mg/L. Figure 4 presents the pyrogram of RE-WWTP showing several peaks corresponding to different organic compounds identified by using the instrument's built-in library database.

Several authors have reported the incomplete removal of a wide range of pollutants in treated wastewater. Although the total organic carbon (TOC) values in the various RE-WWTP samples analyzed in this study ranged from approximately 6 to 12 mg/L, remaining within legally permitted limits, the gradual accumulation of trace levels of organic contaminants, such as pharmaceuticals and plastic-derived compounds, may pose significant environmental and health risks over time.

Numerous studies have confirmed the limited retention of MNPs by conventional wastewater treatment plants (WWTPs) [22]. Among the most commonly detected polymers in municipal effluents are polyester (PES), particularly polyethylene terephthalate (PET) in fiber form, and polyethylene (PE). Other polymers, including polystyrene (PS) and polypropylene (PP), have also been reported [22–24].

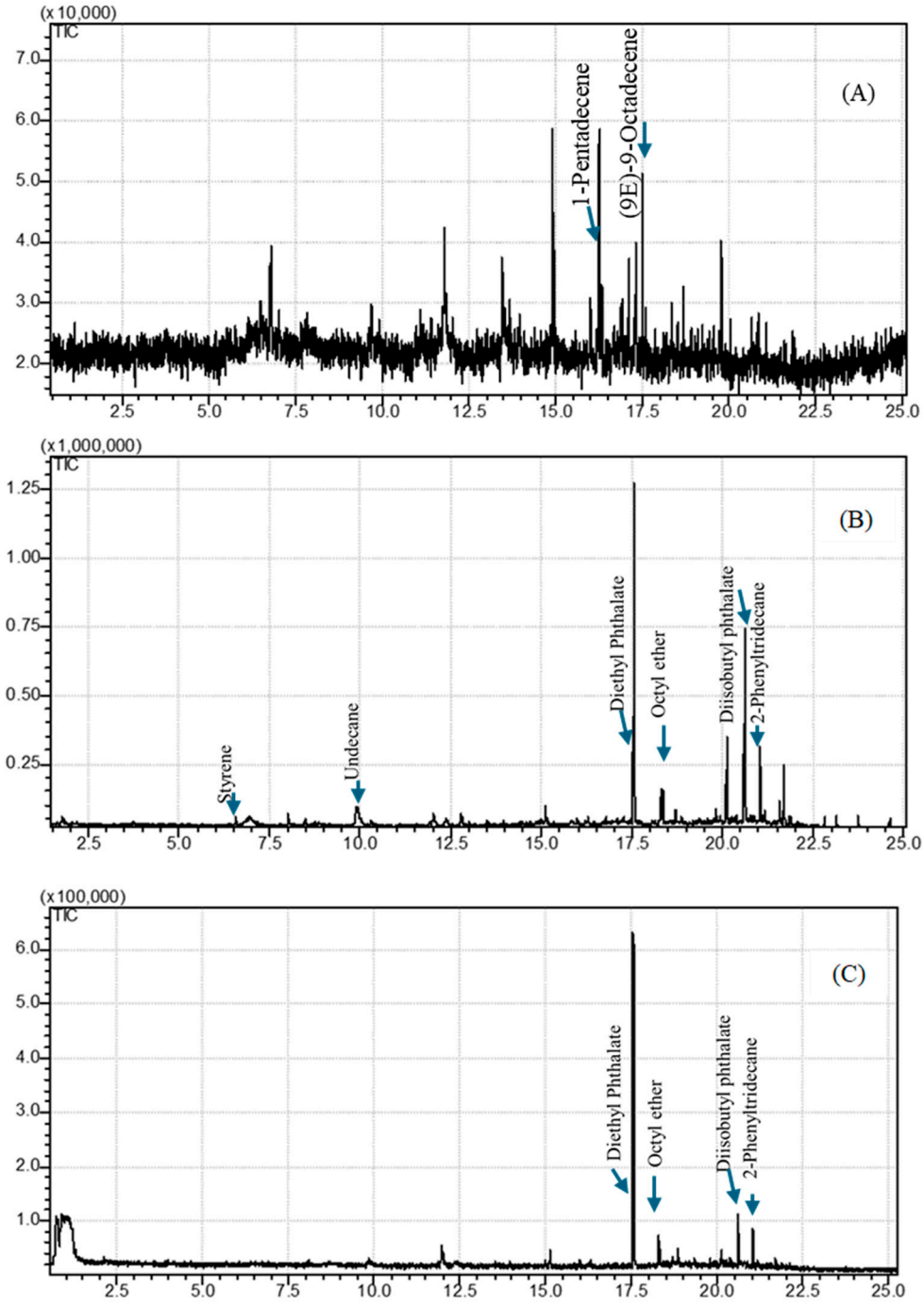

Figure 4. Pyrogram from RE-WWTP analyzed by Py-GC/MS: (**A**) RE-WWTPJ after membrane filtration (0.2 µm), RE-WWTPN (**B**) before and (**C**) after membrane filtration.

Figure 4A shows various peaks; between them, py-GCMS suggested the presence of long-chain alkenes such as 1-pentadecene and 9-octadecene, which are reported as pyrolysis products of polyethylene (PE) [42] and industrial plastic wastes [43], respectively [44]. Their presence suggests the contribution of NP fragments in wastewater as reported by various authors [42,43,45,46]. Figure 4B,C show the results of the Py-GC/MS analysis of the effluent samples, both with and without membrane filtration pretreatment. The analysis suggested the presence of the following organic compounds: diethyl phthalate (DEP), octyl ether, diisobutyl phthalate, and benzene, 1-methyl-dodecyl. These results suggest the potential presence of fragments, byproducts or plasticizers from polyester fibers or other plastics. Phthalic acid esters (PAEs) are common plasticizers added to polymeric materials

to improve their flexibility and workability [47]. Various studies have reported diethyl phthalate (DEP) [30] as the most common phthalate detected in polyester samples [48] and WWTP effluents [49]. Overall, RE-WWTP samples may contain a wide array of organic contaminants, including MNPs, pharmaceuticals, etc., that are often difficult to identify and quantify, due to their complexity and low concentrations. The aim of this work is to explore sustainable and effective methods for degrading and or/mineralizing these compounds to achieve water purification. Among the most promising approaches, photocatalysis is a green technology capable of treating diverse organic pollutants without the use of hazardous reagents.

2.2.2. Real Effluent from Wastewater Treatment Plant Photocatalytic Tests

Photocatalytic tests were conducted on samples of RE-WWTP. Before the tests, a pretreatment step was performed to remove coarse particles through a two-stage membrane filtration: initially using a paper filter with a pore diameter of 5 µm (M1), followed by filtration with a polypropylene membrane with a pore size of 0.2 µm (M2). The effluent with and without pretreatment was taken from the same sample in the same period (November 2024) and showed comparable initial TOC and IC values, suggesting a similar overall organic and inorganic composition with different particles size. The presence of particles retained by the filtration step, was verified by weighing the particles retained by membrane after filtration. Furthermore, the py-GCMS, shown in Figure 4, indicated two small peaks of styrene and undecane in the not-filtered sample. This confirms that differences in particle size distribution and organic compositions are present and may reasonably contribute to the observed differences in degradation rates (Figure 5).

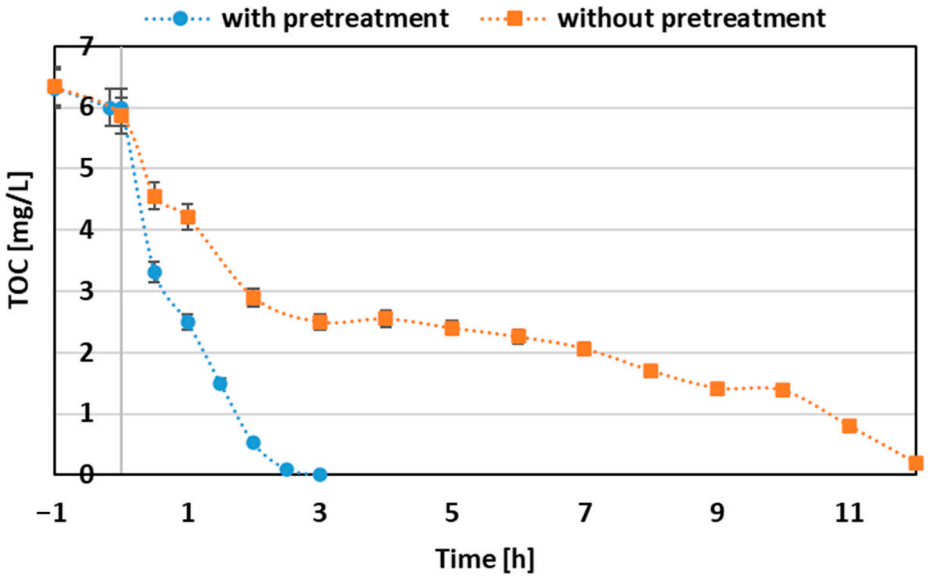

Figure 5. TOC vs. time of RE-WWTPN with and without pretreatment (operative conditions: 500 mL, 1 g/L of TiO_2 as photocatalyst suspension in water, 30 °C, Hg lamp B as irradiation source, oxygen at 0.5 bar as oxidant, all sample were filtered before analysis).

The photocatalytic process represents a green and sustainable approach for enhancing the purification of RE-WWTPs, aiming at the complete mineralization of organic pollutants. Therefore, photocatalytic experiments were carried out on both pretreated and untreated effluent samples. The efficiency of photocatalytic degradation is highly dependent on the composition and size of the organic pollutants present. As shown in our previous studies [24,25,30], small organic molecules, including pharmaceuticals, and some nanoplastics, are generally more reactive in photocatalytic processes due to their higher surface

area-to-volume ratio. This allows for greater interaction with the photocatalyst, leading to more efficient degradation. In contrast, larger particles such as microplastics may degrade more slowly, as their size limits surface exposure and reduces photocatalyst contact.

Furthermore, degradation rates vary depending on the specific chemical nature of the organic compounds present in the effluents. Figure 5 illustrates the mineralization of RE-WWTPN, comparing samples with and without pretreatment. The results indicate that the photocatalytic system is capable of degrading organic substances not removed by conventional municipal treatment processes. Despite the similar and relatively low TOC values, samples without pretreatment required longer reaction times. This is likely due to the presence of larger particles that degrade more slowly, gradually reducing in size over time. Since all samples were filtered prior to TOC analysis at Shimadzu TOC analyzer (to remove residual photocatalyst), the behavior observed in Figure 5 suggests that, during photocatalysis, degrading particles decrease in size to the point where they can pass through the filtration membrane, thus affecting the measured TOC values.

Figure 6 confirms that MNPs and other organic compounds are not detected by Py-GC/MS analysis after 12 h of photocatalytic treatment of RE-WWTPN samples without pretreatment.

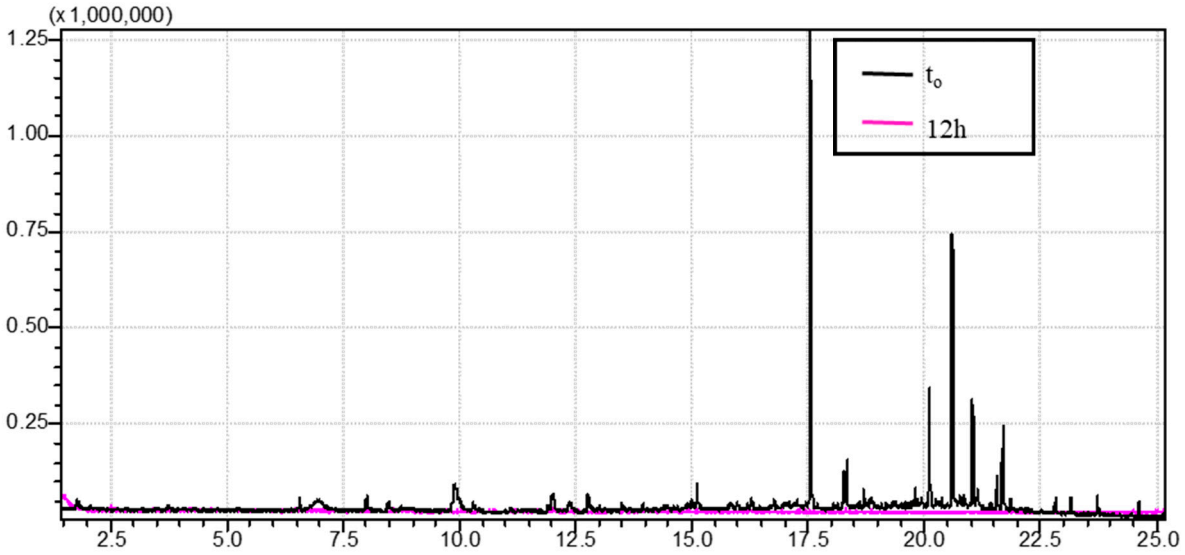

Figure 6. Pyrogram from RE-WWTPN without pretreatment analyzed by Py-GC/MS before and after 12 h of photocatalysis.

Based on the obtained results, further photocatalytic tests were carried out on filtered samples of RE-WWTPN and RE-WWTPJ (Figure 7). Although RE-WWTPN exhibited a lower initial TOC concentration, the time required to obtain a similar degree of mineralization was comparable to that of RE-WWTPJ. This behavior can be attributed to differences in the composition of the organic compounds present in the samples.

Nonetheless, in both cases, the photocatalytic system proved effective in promoting the mineralization of organic contaminants, thereby enhancing the overall purification of the wastewater.

To confirm that the results shown in Figure 7 are due to the presence of the photocatalyst control photolysis tests were performed (Figure S6). The results clearly demonstrated that complete mineralization was achieved only in the presence of TiO_2 confirming the essential role of the photocatalyst in the degradation process.

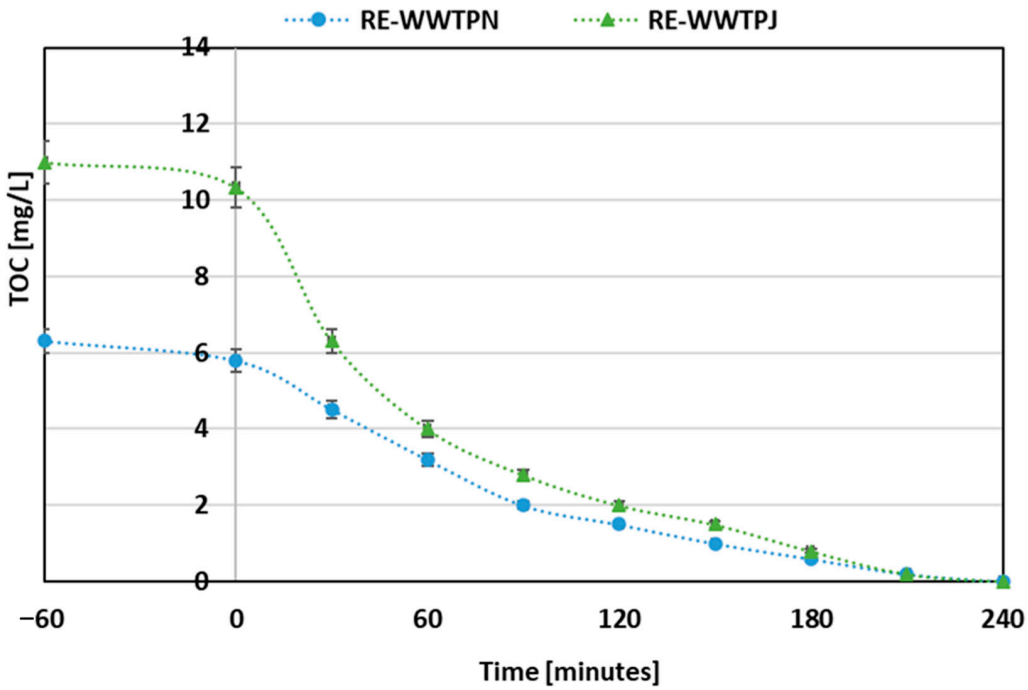

Figure 7. TOC vs. time by using TiO_2 as photocatalyst, oxygen at 0.5 bar as oxidant (operative conditions: 500 mL, 1 g L^{-1} of TiO_2 as photocatalyst suspension in water, 30 °C, Hg lamp B as irradiation source).

2.2.3. Gemfibrozil in Real Effluent from Wastewater Treatment Plant

The concentration of GEM in RE-WWTPs is usually very low making its detection and analysis with certain analytical instruments challenging. Therefore 10 mg/L of GEM was added to RE-WWTPJ mixed with RE-WWTPN (RE-WWTPJN) to obtain an average effluent and simulate the coexistence of both drug and plastic pollutants. The characterization of RE-WWTPJN indicated the possible presence of pollutants such as fragments, monomers, by products or additives of nanoplastics. The matrix in which a substance is present plays a crucial role in its degradation. The degradation process can differ between pure water and real effluent from wastewater treatment plant (WWTP) due to the variation in composition, interactions and environmental factors. For this reason, we investigated the photocatalytic degradation of gemfibrozil (as a model drug) in pure water and RE-WWTPN and RE-WWTPJ mixed (after membrane pretreatment). The results showed similar behavior in terms of complete degradation of gemfibrozil when using real effluent as the matrix; however, mineralization required more time due to the presence of other pollutants, as shown in Figure 8.

2.3. Membrane Characterization

The use of a membrane system coupled with a photocatalytic reactor offers several advantages, as it confines the photocatalyst, the substrate and its oxidation products within the reactive ambient, allowing the treated water to be withdrawn as permeate.

The flow rate and pressure in the permeation cell contained in the PMR (Figure 9) were measured before using the membrane for photocatalytic tests. The NF Fortilife membrane was characterized by determining the permeate flux, expressed as L/m^2 h (LMH). The flow rate characterization was performed with ultrapure water at three different pressures: 6, 5 and 4 bar; the results are reported in Figure 10A, while rejection percentage measured using RE-WWTPJN and GEM is reported in Figure 10B.

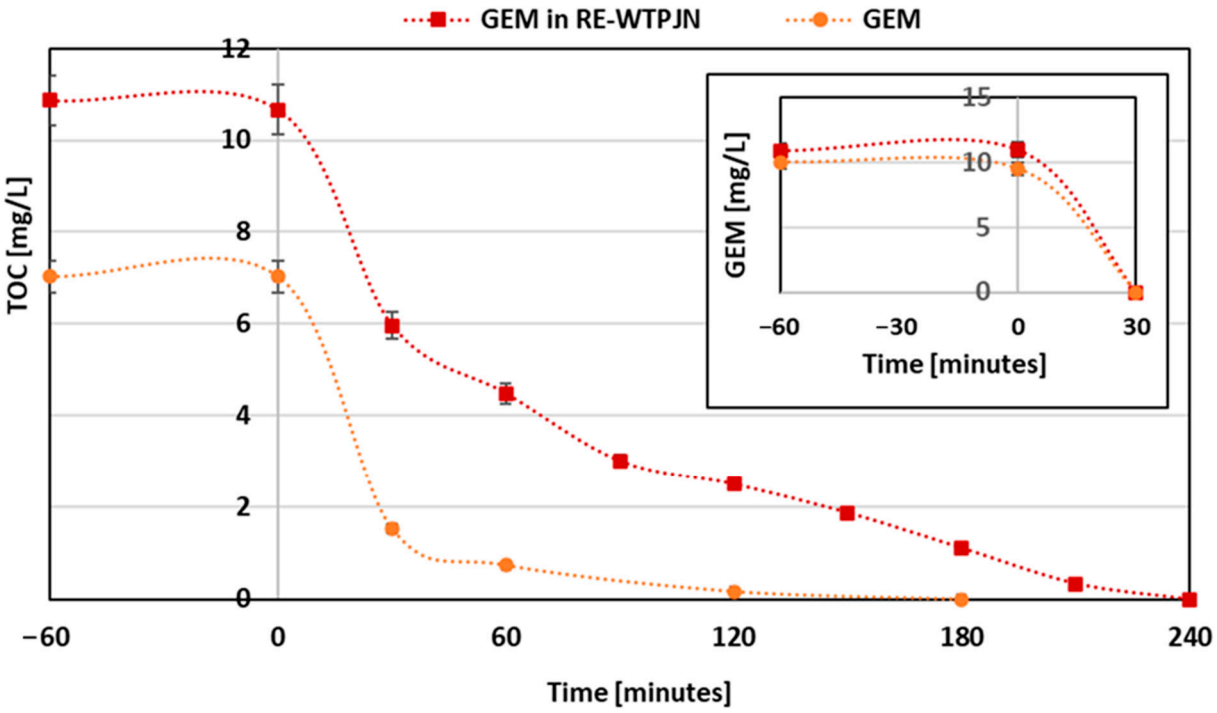

Figure 8. Gemfibrozil mineralization as TOC vs. time in pure water or in RE-WWTPJN. The inset reports the Gemfibrozil concentration vs. time in the same test (operative conditions: 500 mL, 1 g/L of TiO_2 as photocatalyst suspension in water, 30 °C, Hg lamp B as irradiation source, oxygen at 0.5 bar as oxidant).

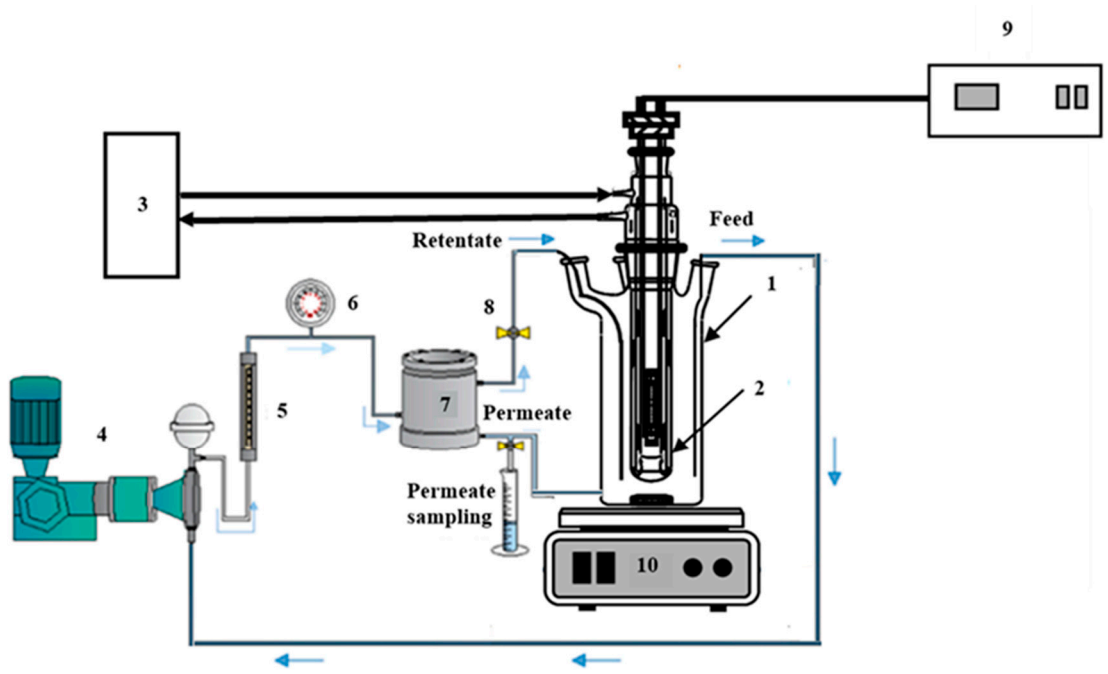

Figure 9. Scheme of the updated experimental setup: (1) photoreactor; (2) medium pressure Hg lamp with cooling jacket; (3) thermostatic bath with cooling water; (4) diaphragm pump; (5) flowmeter; (6) pressure gauge; (7) external membrane cell; (8) pressure valve; (9) power supply; (10) magnetic stirrer.

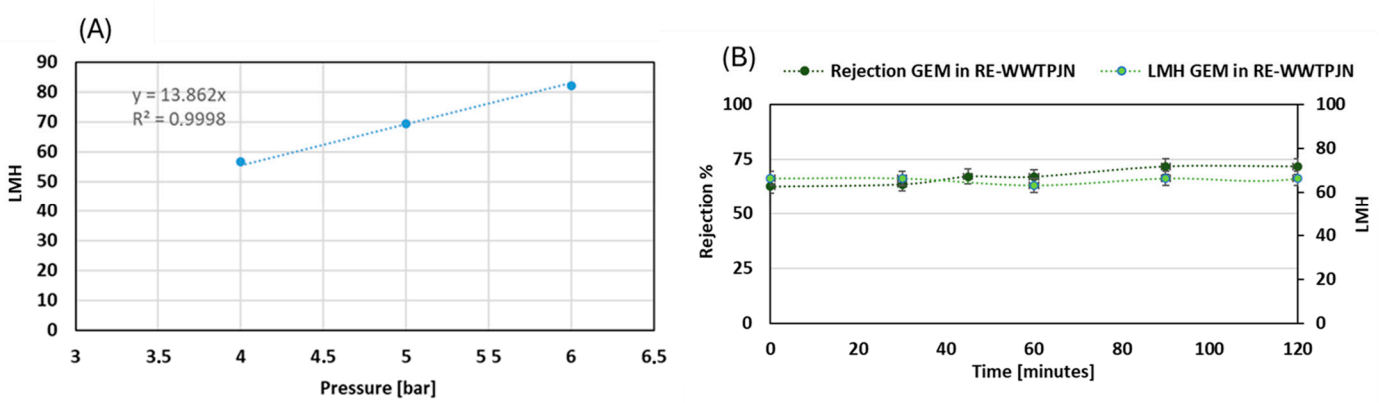

Figure 10. (**A**) Fluxes of ultrapure water of Fortlife membrane vs. time measured at different pressure (6, 5 and 4 bar); (**B**) Gemfibrozil rejection and permeate fluxes vs. times (GEM 10 mg/L in RE-WWTPJN, applied transmembrane pressure 5.0 bar).

Flux and Rejection Tests with GEM in Real Effluent

One advantage in using a membrane process coupled to the photocatalytic system should be retention in the reactive ambient not only of the photocatalyst but also of the pollutants.

To verify the rejection property, tests with GEM solutions at an initial concentration of 10 mg/L in a solution of real effluent were carried out in the same system shown in Figure 9 without photocatalyst and UV light.

The membrane achieved a rejection of about 67% of Gemfibrozil in real effluent. The measured permeate flux (Jp) was 66 L/m^2 h at steady state under a pressure of 5 bar (Figure 9).

2.4. Photocatalytic Mineralization of GEM in Real Effluent in PMR

All photocatalytic tests shown before indicated that the photocatalytic system can improve the treatment of WWTPTs for the removal of recalcitrant pollutants, including nanoplastics, from wastewater. For practical application, it is crucial to ensure that the photocatalyst remains within the reactive environment. Figure 11 shows the photocatalytic degradation of GEM in RE-WWTPJL in the PMR described in Figure 9 where the photocatalyst is in suspension and retained by the membrane.

The results demonstrated that GEM was completely degraded after 1 h, while complete mineralization of all pollutants was achieved after 5 h of photocatalytic treatment. The permeate flowrate was measured by recording the volume of permeate over time. Its relatively constant trend indicates that, under these operating conditions, the membrane contactor did not exhibit significant fouling issues. The filtration prior to the photocatalysis run improved the photocatalytic rate and reduced the possible fouling formation due to coarse particles.

The longer degradation time observed in the PMR compared to the batch system can be mainly attributed to limited light exposure. In the PMR, the presence of unirradiated zones, such as tubing and membrane compartments, reduces the effective volume exposed to UV light, which in turn limits the photocatalytic efficiency.

Additionally, although TiO_2 is retained by the nanofiltration (NF) membrane and remains in the reactive zone, it may not be uniformly irradiated throughout the reactor. Photocatalyst particles can become unevenly distributed, particularly near the membrane surface, where reduced turbulence or flow stagnation may lead to local accumulation. In these regions, the photocatalyst might receive insufficient UV irradiation lowering the generation of reactive species and slowing down the degradation of adsorbed pollutants like GEM.

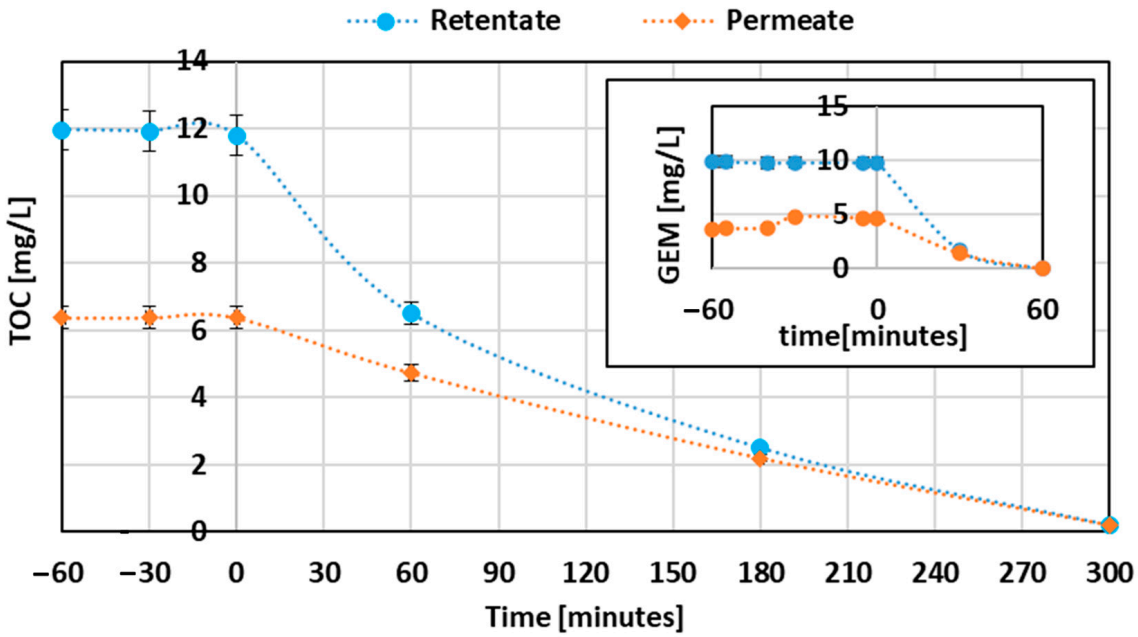

Figure 11. Gemfibrozil mineralization as TOC vs. time in PMR (retentate and permeate). The inset reports the GEM concentration vs. time in the same test (operative conditions: 800 mL, 1 g/L of TiO_2 as photocatalyst suspension in water, 30 °C, Hg lamp as irradiation source, oxygen at 0.5 bar as oxidant, GEM 10 mg/L in RE-WWTPJN).

This issue can be mitigated by increasing tangential flow within the permeation cell to improve catalyst dispersion and reduce dead zones, or by optimizing the PMR configuration as reported in our previous works [11,25,50] to ensure more uniform irradiation and flow dynamics.

Building on these findings, this study proposes the integration of a PMR as an advanced tertiary treatment stage in WWTPs to significantly enhance effluent quality. The system is designed to retain the photocatalyst within the reactive zone, enabling the continuous recirculation of non-degraded pollutants until complete mineralization is achieved.

Figure 12 illustrates the proposed configuration, in which the PMR treats secondary effluent containing residual organic contaminants such as pharmaceuticals and micro/nanoplastics (MNPs). Through the combination of photocatalysis and membrane separation, all organic carbon is progressively degraded, leading to the production of a high-quality effluent that can be safely discharged into the environment.

The nanofiltration membrane within the PMR plays a dual role: it confines both the photocatalyst and the pollutants within the reactive volume, thereby maximizing contact with the UV-irradiated catalyst, and allows only fully treated water to pass through as permeate. This ensures that emerging contaminants, including those not removed during conventional biological treatment, are effectively degraded within the reactor.

This integrated approach represents a promising strategy for the removal of persistent organic pollutants and plastic residues from municipal wastewater, addressing growing concerns regarding their environmental and health impacts.

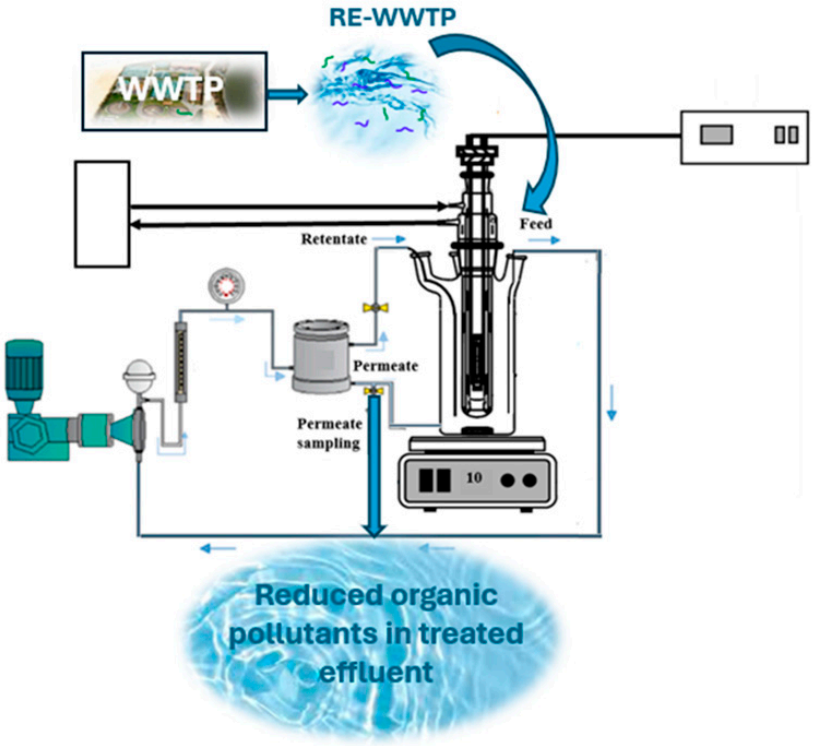

Figure 12. Scheme of improvements of the WWTP for its purification from organic pollutants.

3. Experimental Section

3.1. Materials

Titanium dioxide (TiO_2) P25 type from Evonic-Degussa (crystallographic phase ca. 80% anatase and 20% rutile, band gap 3.2 eV); Tungsten oxide (WO_3), 99.9% (metals basis) band gap 2.5–2.7 eV [51] and Niobium(V) oxide (Nb_2O_5), 99.9% (metals basis) band gap ~3.4 eV [41] from Alfa Aesar were used as photocatalysts. Gemfibrozil (GEM), sourced from Sigma, was selected as the reference contaminant. Chemically identified as 5-(2,5-dimethylphenoxy)-2,2-dimethylpentanoic acid, this compound belongs to the fibrate class of lipid-lowering agents. Its molecular formula is $C_{15}H_{22}O_3$ with a molecular weight of 250.35 g/mol. Aqueous GEM solutions were obtained by dissolving 10 mg of the compound in one liter of ultrapure water, adjusting the pH to 9.7. To remove the photocatalyst before analysis a flat sheet hydrophilic microfiltration porous polypropylene membrane (GH-Polypro, Pall Corporation) with a pore size 0.2 μm was used. A Polypiperazine thin-film composite membrane (commercial flat sheet nanofiltration membrane FilmTec™ Fortilife™ XC-N (DuPont, São Paulo, SP, Brazil)) was used in the membrane cell of the PMR.

Preliminary photocatalytic tests were performed using four irradiation sources: (i) two immersed medium-pressure mercury lamps (125 W, Helios Italquartz, Cambiago, Milan, Italy), referred to as lamps A and B, with maximum emission peaks at 360 nm and light intensities of 4785 μW/cm^2 and 7246 μW/cm^2, respectively (the emission spectrum is reported in Figure S1); (ii) a custom-made immersed UV LED lamp, assembled using LEDs within the same housing as the other lamps, with an emission peak at 367 nm and a light intensity of 105.59 μW/cm^2, as shown in Figure S2; and (iii) TUV TL Mini lamps UVC (2.73 μw/cm^2) with the emission peak at 250 nm (Figure S3).

3.2. Instrumental and Analytical Methods

Samples of gemfibrozil and RE-WWTP were taken from the solution during all photocatalytic tests and characterized by TOC. Before analysis, the samples were filtered with a GH-Polypro membrane to eliminate the photocatalyst particles.

To detect GEM concentration, a high-performance liquid chromatography (HPLC, Thermo Scientific UltiMate 3000 HPLC system) was used with a Phenomenex Synergi 4u Fusion-RP 80A (Phenomenex, Torrance, CA, USA, 4.60 mm × 250 mm, 4 μm) column by UV readings at 220 nm wavelength. An acetonitrile/phosphate buffer at pH 3.1 solution 70/30 (*v*/*v*) was used as mobile phase fed to a flow rate of 1.0 mL/min. The injection volume was 20 μL and the column pressure was 98 bar.

Real effluent from wastewater treatment plant or Gemfibrozil mineralization were analyzed by total organic carbon (TOC) measurements, performed by using a TOC-VCSN from Shimadzu (Shimadzu, Kyoto, Japan).

A pH meter (WTW Inolab Terminal Level 3, Weilheim, Germany)) with a glass pH-electrode SenTix 81 (WTW) was used for pH measurements. The irradiance of all lamps was measured using a radiometer (UVX radiometer UVP, Upland, CA, USA)) placed in direct contact with the external surface of the reactor. All measurements were taken at the same fixed distance to ensure comparability.

Py-GC/MS was used to analyze the composition of a real effluent from the wastewater treatment plant. Samples (20 μL) were pyrolyzed at 600 °C. Pyrolysis products were injected with a split of 20, on a Py-GC/MS device (Shimadzu, Kyoto, Japan). Temperatures of the pyrolyzer interface and the pyrolyzer furnace were set at 300 °C and 600 °C, respectively. Helium was used as a carrier gas with a linear velocity of 36.1 cm/min. The initial oven program was set as follows: 40 °C for 2 min, then increased to 320 °C at 10 °C/min, and maintained for 16 min.

3.3. Experimental Apparatus

3.3.1. Batch Photoreactor

The preliminary experimental tests on photocatalytic degradation of Gemfibrozil were conducted in a cylindrical Pyrex glass reactor with a volume of 500 mL reported in Figure S4 with one of the following immersed lamps:

- Hg lamp A;
- Hg lamp B;
- LED lamp 367 nm;
- TUV TL Mini lamps UVC.

The reactor was equipped with 3 outputs in the top section for sampling the suspension, for blowing oxygen and for its degassing. The lamp was positioned axially inside the reactor and the circulation of distilled water in the Pyrex glass jacket surrounding it allowed us to maintain the system at a temperature of 30 °C. The solution was submitted to agitation using a magnetic stirrer.

3.3.2. Photocatalytic Membrane Reactor

Photocatalytic reactions were carried out also in the PMR shown in Figure 9. In this configuration, both the retentate and permeate streams were continuously recycled back into the photoreactor. The external flat-sheet membrane was housed in a stainless-steel cylindrical cell designed to operate under pressure. The nanofiltration membrane, with an active surface area of 19 cm^2, was positioned on a porous sintered stainless-steel disk located at the bottom of the cell. The cell, with a total volume of 95 mL, was pressurized using a diaphragm pump.

Membrane permeability and rejection experiments were conducted using ultrapure water and a real effluent from a wastewater treatment plant (RE-WWTP) spiked with 10 mg/L of gemfibrozil (GEM), respectively. The experimental setup was the same as that shown in Figure 9. The permeate flow rate over time was determined by collecting fixed volumes at regular intervals. Rejection efficiency (R%) was calculated based on the GEM concentrations measured by HPLC, using the following equation: $R\% = (1 - (Cp/Cr)) \times 100$, where Cp and Cr are the concentrations of the drug present in the permeate and in the retentate, respectively.

3.3.3. Photocatalytic Tests

To optimize the operative conditions for photocatalytic degradation of gemfibrozil and of the organic molecules present in the real effluent from wastewater treatment plant, experimental tests were conducted in batch reactor with a volume of 500 mL, shown in Figure S4, with water as solvent. All photocatalytic tests were carried out by mixing the photocatalyst with 10 mg/L of gemfibrozil or with the effluent for 60 min before to switch-on light irradiation to allow the adsorption of the substrate on the photocatalyst. The temperature was constant at 30 °C.

4. Conclusions

This study highlighted the potential of photocatalytic processes to enhance the purification of effluents from WWTPs. Photocatalytic degradation experiments were carried out on various emerging pollutants using both real and simulated WWTP effluents. GEM was selected as a model contaminant to evaluate the effects of key operational parameters, including photocatalyst type, irradiation source, and oxidant.

The most effective conditions were achieved using TiO_2 as the photocatalyst, a medium-pressure UV mercury lamp as the irradiation source, and oxygen as the oxidant in a batch photoreactor. Under these conditions, complete mineralization of the GEM and all organic compounds present in the real effluent was achieved within 4 h.

Chemical characterization of real WWTP effluent samples indicated the presence of organic compounds such as plastic additives (e.g., phthalate), likely associated with MNPs. Photocatalytic treatment, both with and without membrane integration, was effective in achieving complete mineralization of these compounds. However, in view of practical applications, the ability to confine the photocatalyst within the reactive zone, as well as retaining the not photodegraded pollutants, is a crucial aspect. Therefore, additional experiments were performed in a photocatalytic membrane reactor (PMR), confirming its suitability for maintaining the catalyst in suspension and enabling pollutant degradation in a continuous process. Application of the PMR to real wastewater effluents, both filtered and unfiltered, spiked and unspiked with gemfibrozil, enabled a comprehensive and practically relevant evaluation of performance under real-world conditions. The filtration prior to photocatalysis improved the photocatalytic rate and reduced the possible membrane fouling due to coarse particles.

Overall, photocatalytic oxidation proves to be a promising and versatile approach for the removal of persistent organic pollutants, including pharmaceuticals and plastic-related contaminants. Further research should focus on optimizing this technology for integration into the tertiary treatment stage of WWTPs, with the goal of achieving complete water purification and safe environmental discharge.

Supplementary Materials: The following supporting information can be downloaded at: https://www.mdpi.com/article/10.3390/catal15090904/s1, Figure S1: Emission spectrum of UV lamp; Figure S2: Emission Spectrum of the LED immersed lamp with emission peak at 367 nm; Figure S3: Emission Spectrum of the TUV TL Mini lamps UVC; Figure S4: Scheme of the 500 mL batch photoreac-

tor: (a) oxygen cylinder; (b) photoreactor; (c) medium pressure Hg lamp with cooling jacket/UV LED lamp/TUV TL Mini lamps UVC; (d) power supply; (e) magnetic stirrer; (f) thermostatic bath with cooling water; (g) sampling valve; (h) degassing system; (MF) samples microfiltration; (HPLC) HPLC analyses; Figure S5: TOC vs. time by irradiating with the 4 lamps without photocatalyst (operative conditions: 500 mL, 10 g/L Gemfibrozil 30 °C oxygen pressure 0.5 bar); Figure S6: TOC/TOC0 of the real effluent from wastewater treatment plant vs. time without photocatalyst by irradiating with Hg lamp as irradiation source (operative conditions: 500 mL, 30 °C).

Author Contributions: C.L.: conceptualization, investigation, supervision, writing—original draft, review and editing. A.S.: investigation. P.A.: supervision, review and editing. R.M.: conceptualization, supervision, review and editing, funding acquisition. B.R.: review and editing, A.F.: review and editing, funding acquisition. T.P.: conceptualization, supervision, writing—review and editing, funding acquisition. All authors have read and agreed to the published version of the manuscript.

Funding: This research received financial support through the project "Tech4You_Technologies for Climate Change Adaptation and Quality of Life Improvement"_National Recovery and Resilience Plan (NRRP), Mission 4, Component 2, Investment 1.5, funded by the European Union−NextGeneration EU, Identity code: ECS 00000009, CUP B83C22003980006; CUP H23C22000370006.

Data Availability Statement: Data will be made available on request.

Acknowledgments: A.S. thanks the above "Tech4You" project for funding her doctorate fellowship. C.L. also thanks this project for funding her Research Grant.

Conflicts of Interest: The authors declare no conflicts of interest.

References

1. Gatidou, G.; Arvaniti, O.S.; Stasinakis, A.S. Review on the occurrence and fate of microplastics in Sewage Treatment Plants. *J. Hazard. Mater.* **2019**, *367*, 504–512. [CrossRef] [PubMed]
2. Deng, S.; Hu, J.; Ong, S.-L.; Li, Q.; Han, J. Advanced technologies for industrial wastewater reclamation. *Front. Environ. Sci.* **2023**, *11*, 542. [CrossRef]
3. Singh, B.J.; Chakraborty, A.; Sehgal, R. A systematic review of industrial wastewater management: Evaluating challenges and enablers. *J. Environ. Manag.* **2023**, *348*, 119230. [CrossRef]
4. Toray Membrane USA. Optimizing RO-Membrane Performance in Produced-Water Applications. Available online: https://www.wateronline.com/doc/optimizing-ro-membrane-performance-in-produced-water-applications-0001?vm_tId=2518845&vm_nId=80299&user=0038f1ed-66e0-46bd-91e2-ebaf82420db6&gdpr=1&vm_alias=O (accessed on 14 July 2023).
5. Cacace, D.; Fatta-Kassinos, D.; Manaia, C.M.; Cytryn, E.; Kreuzinger, N.; Rizzo, L.; Karaolia, P.; Schwartz, T.; Alexander, J.; Merlin, C.; et al. Antibiotic resistance genes in treated wastewater and in the receiving water bodies: A pan-European survey of urban settings. *Water Res.* **2019**, *162*, 320–330. [CrossRef]
6. Corno, G.; Yang, Y.; Eckert, E.M.; Fontaneto, D.; Fiorentino, A.; Galafassi, S.; Zhang, T.; Di Cesare, A. Effluents of wastewater treatment plants promote the rapid stabilization of the antibiotic resistome in receiving freshwater bodies. *Water Res.* **2019**, *158*, 72–81. [CrossRef]
7. Manaia, C.M.; Rocha, J.; Scaccia, N.; Marano, R.; Radu, E.; Biancullo, F.; Cerqueira, F.; Fortunato, G.; Iakovides, I.C.; Zammit, I.; et al. Antibiotic resistance in wastewater treatment plants: Tackling the black box. *Environ. Int.* **2018**, *115*, 312–324. [CrossRef] [PubMed]
8. Osińska, A.; Korzeniewska, E.; Harnisz, M.; Felis, E.; Bajkacz, S.; Jachimowicz, P.; Niestępski, S.; Konopka, I. Small-scale wastewater treatment plants as a source of the dissemination of antibiotic resistance genes in the aquatic environment. *J. Hazard. Mater.* **2020**, *381*, 121221. [CrossRef]
9. Monira, S.; Roychand, R.; Hai, F.I.; Bhuiyan, M.; Dhar, B.R.; Pramanik, B.K. Nano and microplastics occurrence in wastewater treatment plants: A comprehensive understanding of microplastics fragmentation and their removal. *Chemosphere* **2023**, *334*, 139011. [CrossRef]
10. Koyuncuoğlu, P.; Erden, G. Microplastics in municipal wastewater treatment plants: A case study of Denizli/Turkey. *Front. Environ. Sci. Eng.* **2023**, *17*, 99. [CrossRef]
11. Russo, B.; Lavorato, C.; Argurio, P.; Limonti, C.; Siciliano, A.; Figoli, A.; Poerio, T. Nanofiltration as an effective tertiary treatment for the removal of micro-and nanoplastics from municipal water effluent. *Sep. Purif. Technol.* **2025**, *376*, 134121. [CrossRef]
12. Wang, C.; Wang, J.; Gao, W.; Ning, X.; Xu, S.; Wang, X.; Chu, J.; Ma, S.; Bai, Z.; Yue, G.; et al. The fate of phthalate acid esters in wastewater treatment plants and their impact on receiving waters. *Sci. Total Environ.* **2023**, *873*, 162201. [CrossRef] [PubMed]

13. Smith, M.; Love, D.C.; Rochman, C.M.; Neff, R.A. Microplastics in seafood and the implications for human health. *Curr. Environ. Health Rep.* **2018**, *5*, 375–386. [CrossRef]
14. Wright, S.L.; Kelly, F.J. Plastic and human health: A micro issue? *Environ. Sci. Technol.* **2017**, *51*, 6634–6647. [CrossRef]
15. Campanale, C.; Massarelli, C.; Savino, I.; Locaputo, V.; Uricchio, V.F. A Detailed Review Study on Potential Effects of Microplastics and Additives of Concern on Human Health. *Int. J. Environ. Res. Public Health* **2020**, *17*, 1212. [CrossRef]
16. Prata, J.C.; Silva, A.L.P.; Da Costa, J.P.; Mouneyrac, C.; Walker, T.R.; Duarte, A.C.; Rocha-Santos, T. Solutions and integrated strategies for the control and mitigation of plastic and microplastic pollution. *Int. J. Environ. Res. Public Health* **2019**, *16*, 2411. [CrossRef] [PubMed]
17. Souza, A.M.d.; Santos, A.L.; Araújo, D.S.; Magalhães, R.R.d.B.; Rocha, T.L. Micro(nano)plastics as a vector of pharmaceuticals in aquatic ecosystem: Historical review and future trends. *J. Hazard. Mater. Adv.* **2022**, *6*, 100068. [CrossRef]
18. Rochman, C.M.; Hoh, E.; Kurobe, T.; Teh, S.J. Ingested plastic transfers hazardous chemicals to fish and induces hepatic stress. *Sci. Rep.* **2013**, *3*, 3263. [CrossRef]
19. Fang, Y.; Karnjanapiboonwong, A.; Chase, D.A.; Wang, J.; Morse, A.N.; Anderson, T.A. Occurrence, fate, and persistence of gemfibrozil in water and soil. *Environ. Toxicol. Chem.* **2012**, *31*, 550–555. [CrossRef]
20. Grenni, P.; Patrolecco, L.; Ademollo, N.; Di Lenola, M.; Barra Caracciolo, A. Assessment of gemfibrozil persistence in river water alone and in co-presence of naproxen. *Microchem. J.* **2018**, *136*, 49–55. [CrossRef]
21. Grenni, P.; Patrolecco, L.; Ademollo, N.; Tolomei, A.; Barra Caracciolo, A. Degradation of Gemfibrozil and Naproxen in a river water ecosystem. *Microchem. J.* **2013**, *107*, 158–164. [CrossRef]
22. Gómez-Regalado, M.d.C.; Martín, J.; Santos, J.L.; Aparicio, I.; Alonso, E.; Zafra-Gómez, A. Bioaccumulation/bioconcentration of pharmaceutical active compounds in aquatic organisms: Assessment and factors database. *Sci. Total Environ.* **2023**, *861*, 160638. [CrossRef] [PubMed]
23. Molinari, R.; Severino, A.; Lavorato, C.; Argurio, P. Which Configuration of Photocatalytic Membrane Reactors Has a Major Potential to Be Used at an Industrial Level in Tertiary Sewage Wastewater Treatment? *Catalysts* **2023**, *13*, 1204. [CrossRef]
24. Severino, A.; Russo, B.; Lavorato, C.; Argurio, P.; Figoli, A.; Molinari, R.; Poerio, T. Integrated nanofiltration and photocatalytic processes for the removal of polystyrene nanoplastics waste in water. *Sep. Purif. Technol.* **2025**, *360*, 131232. [CrossRef]
25. Molinari, R.; Limonti, C.; Lavorato, C.; Siciliano, A.; Argurio, P. Upgrade of a slurry photocatalytic membrane reactor based on a vertical filter and an external membrane and testing in the photodegradation of a model pollutant in water. *Chem. Eng. J.* **2023**, *451*, 138577. [CrossRef]
26. Molinari, R.; Lavorato, C.; Argurio, P. The Evolution of Photocatalytic Membrane Reactors over the Last 20 Years: A State of the Art Perspective. *Catalysts* **2021**, *11*, 775. [CrossRef]
27. Mastropietro, T.F.; Meringolo, C.; Poerio, T.; Scarpelli, F.; Godbert, N.; Di Profio, G.; Fontananova, E. Multistimuli Activation of TiO_2/α-Alumina Membranes for Degradation of Methylene Blue. *Ind. Eng. Chem. Res.* **2017**, *56*, 11049–11057. [CrossRef]
28. Roy, J.S.; Messaddeq, Y. The Role of Solar Concentrators in Photocatalytic Wastewater Treatment. *Energies* **2024**, *17*, 4001. [CrossRef]
29. Close, J.; Ip, J.; Lam, K.H. Water recycling with PV-powered UV-LED disinfection. *Renew. Energy* **2006**, *31*, 1657–1664. [CrossRef]
30. Poerio, T.; Lavorato, C.; Severino, A.; Russo, B.; Molinari, R.; Argurio, P.; Figoli, A. Combined membrane separation and photocatalysis process for the recovery and decomposition of micro/nanoplastics from polyester fabrics. *J. Environ. Chem. Eng.* **2024**, *12*, 113310. [CrossRef]
31. Severino, A.; Grirrane, A.; Cabrero-Antonino, M.; Lavorato, C.; Argurio, P.; Molinari, R.; García, H. Visible-Light-Driven Photocatalytic Hydrogen Production from Polystyrene Nanoplastics Using Pd/TiO_2 Nanoparticles. *ACS Appl. Nano Mater.* **2025**, *8*, 14720–14732. [CrossRef]
32. Ghorbani, A.; Bayati, B.; Poerio, T.; Argurio, P.; Kikhavani, T.; Namdari, M.; Ferreira, L.M. Application of NF Polymeric Membranes for Removal of Multicomponent Heat-Stable Salts (HSS) Ions from Methyl Diethanolamine (MDEA) Solutions. *Molecules* **2020**, *25*, 4911. [CrossRef]
33. Mastropietro, T.F.; Drioli, E.; Candamano, S.; Poerio, T. Crystallization and assembling of FAU nanozeolites on porous ceramic supports for zeolite membrane synthesis. *Microporous Mesoporous Mater.* **2016**, *228*, 141–146. [CrossRef]
34. Molinari, R.; Argurio, P.; Poerio, T.; Gullone, G. Selective separation of copper(II) and nickel(II) from aqueous systems by polymer assisted ultrafiltration. *Desalination* **2006**, *200*, 728–730. [CrossRef]
35. Molinari, R.; Lavorato, C.; Argurio, P. Visible-Light Photocatalysts and Their Perspectives for Building Photocatalytic Membrane Reactors for Various Liquid Phase Chemical Conversions. *Catalysts* **2020**, *10*, 1334. [CrossRef]
36. Poerio, T.; Denisi, T.; Mazzei, R.; Bazzarelli, F.; Piacentini, E.; Giorno, L.; Curcio, E. Identification of fouling mechanisms in cross-flow microfiltration of olive-mills wastewater. *J. Water Process Eng.* **2022**, *49*, 103058. [CrossRef]
37. Souza, R.P.; Freitas, T.K.F.S.; Domingues, F.S.; Pezoti, O.; Ambrosio, E.; Ferrari-Lima, A.M.; Garcia, J.C. Photocatalytic activity of TiO_2, ZnO and Nb_2O_5 applied to degradation of textile wastewater. *J. Photochem. Photobiol. A Chem.* **2016**, *329*, 9–17. [CrossRef]

38. Ni, Z.; Wang, Q.; Guo, Y.; Liu, H.; Zhang, Q. Research Progress of Tungsten Oxide-Based Catalysts in Photocatalytic Reactions. *Catalysts* **2023**, *13*, 579. [CrossRef]
39. Gatou, M.-A.; Syrrakou, A.; Lagopati, N.; Pavlatou, E.A. Photocatalytic TiO_2-Based Nanostructures as a Promising Material for Diverse Environmental Applications: A Review. *Reactions* **2024**, *5*, 135–194. [CrossRef]
40. Chen, S.; Xiao, Y.; Xie, W.; Wang, Y.; Hu, Z.; Zhang, W.; Zhao, H. Facile Strategy for Synthesizing Non-Stoichiometric Monoclinic Structured Tungsten Trioxide (WO_{3-x}) with Plasma Resonance Absorption and Enhanced Photocatalytic Activity. *Nanomaterials* **2018**, *8*, 553. [CrossRef]
41. Fuziki, M.E.K.; Ribas, L.S.; Abreu, E.; Fernandes, L.; dos Santos, O.A.A.; Brackmann, R.; de Tuesta, J.L.D.; Tusset, A.M.; Lenzi, G.G. N-Doped TiO_2-Nb_2O_5 Sol–Gel catalysts: Synthesis, characterization, adsorption capacity, photocatalytic and antioxidant activity. *Catalysts* **2023**, *13*, 1233. [CrossRef]
42. Steinmetz, Z.; Kintzi, A.; Muñoz, K.; Schaumann, G.E. A simple method for the selective quantification of polyethylene, polypropylene, and polystyrene plastic debris in soil by pyrolysis-gas chromatography/mass spectrometry. *J. Anal. Appl. Pyrolysis* **2020**, *147*, 104803. [CrossRef]
43. Kohli, K.; Chandrasekaran, S.R.; Prajapati, R.; Kunwar, B.; Al-Salem, S.; Moser, B.R.; Sharma, B.K. Pyrolytic depolymerization mechanisms for post-consumer plastic wastes. *Energies* **2022**, *15*, 8821. [CrossRef]
44. Onwudili, J.A.; Insura, N.; Williams, P.T. Composition of products from the pyrolysis of polyethylene and polystyrene in a closed batch reactor: Effects of temperature and residence time. *J. Anal. Appl. Pyrolysis* **2009**, *86*, 293–303. [CrossRef]
45. Santos, L.H.; Insa, S.; Arxé, M.; Buttiglieri, G.; Rodríguez-Mozaz, S.; Barceló, D. Analysis of microplastics in the environment: Identification and quantification of trace levels of common types of plastic polymers using pyrolysis-GC/MS. *MethodsX* **2023**, *10*, 102143. [CrossRef] [PubMed]
46. Zhou, Y.; Fu, B.; Che, J.; Ye, X. Simultaneous Determination of Six Common Microplastics by a Domestic Py-GC/MS. *Atmosphere* **2025**, *16*, 476. [CrossRef]
47. Huang, L.; Zhu, X.; Zhou, S.; Cheng, Z.; Shi, K.; Zhang, C.; Shao, H. Phthalic Acid Esters: Natural Sources and Biological Activities. *Toxins* **2021**, *13*, 495. [CrossRef]
48. Forakis, J.; Lynch, J. Pyrolysis-GC/MS differentiates polyesters and detects additives for improved monitoring of textile labeling accuracy and plastic pollution. *Anal. Bioanal. Chem.* **2025**, *417*, 3113–3126. [CrossRef]
49. Kotowska, U.; Kapelewska, J.; Sawczuk, R. Occurrence, removal, and environmental risk of phthalates in wastewaters, landfill leachates, and groundwater in Poland. *Environ. Pollut.* **2020**, *267*, 115643. [CrossRef] [PubMed]
50. Molinari, R.; Caruso, A.; Argurio, P.; Poerio, T. Degradation of the drugs Gemfibrozil and Tamoxifen in pressurized and de-pressurized membrane photoreactors using suspended polycrystalline TiO_2 as catalyst. *J. Membr. Sci.* **2008**, *319*, 54–63. [CrossRef]
51. Shandilya, P.; Sambyal, S.; Sharma, R.; Mandyal, P.; Fang, B. Properties, optimized morphologies, and advanced strategies for photocatalytic applications of WO_3 based photocatalysts. *J. Hazard. Mater.* **2022**, *428*, 128218. [CrossRef]

Disclaimer/Publisher's Note: The statements, opinions and data contained in all publications are solely those of the individual author(s) and contributor(s) and not of MDPI and/or the editor(s). MDPI and/or the editor(s) disclaim responsibility for any injury to people or property resulting from any ideas, methods, instructions or products referred to in the content.